HHS Public Access

Author manuscript

*Proc IEEE Int Symp Biomed Imaging*. Author manuscript; available in PMC 2017 May 04.

Published in final edited form as:

*Proc IEEE Int Symp Biomed Imaging*. 2016 April ; 2016: 876–880. doi:10.1109/ISBI.2016.7493405.

# Evaluation of Numerical Techniques for Solving the Current Injection Problem in Biological Tissues

**Damon E. Hyde**[1], **Moritz Dannhauer**[2,3], **Simon K. Warfield**[1], **Rob MacLeod**[2,3], and **Dana H. Brooks.**[3,4]

[1]Boston Children's Hospital and Harvard Medical School, Boston MA, 02115 USA

[2]SCI Institute, University of Utah, Salt Lake City, UT, 84112, USA

[3]Center for Integrative Biomedical Computing, University of Utah, Salt Lake City, UT, 84112, USA

[4]ECE Department, Northeastern University, Boston, MA, 02115, USA

## Abstract

Accurate computational modeling of electric fields in the human head has become important in clinical research to study or influence brain functionality. While existing numerical approaches have been evaluated against simple geometries with known closed form solutions, the relationship between these approaches in more complex geometries has not been studied. Here, we compare the three most commonly used approaches for bioelectric modeling: the finite element method (FEM), the finite difference method (FDM), and the boundary element method (BEM). Using both isotropic and anisotropic conductivity distributions, we construct and compare bioelectric models for a realistic head geometry. Our results suggest that both FEM and FDM are capable of accurately model voltages in the brain, while computations from BEM result in significantly larger errors, due to the increased simplicity and implicit model assumptions.

### Index Terms

Transcranial low-current stimulation; TDCS; EEG; source localization; head model; BEM; FDM; FEM

## 1. Introduction

Accurate bioelectric modeling of head tissue is a crucial component of modern diagnostic and therapeutic tools based on the measurement and control of electric fields in the human brain. Non-invasive electrode measurements of scalp voltages with electroencephalography (EEG) are commonly used to study brain activity and reconstruct cortical current sources [1] originating from epileptic brain activity or other neurological diseases [2]. Conversely, scalp electrodes can also be employed to inject low-amplitude currents that modify voltage fields in the human head and modulate brain functionality (transcranial current stimulation (TCS), e.g., [3, 4]). In particular, accurate solution of the current injection problem [5, 6, 4, 7] is crucial for both clinical pre-surgical planning [2], and therapeutic applications [8]. Current injection directly models TCS and also provides the basis for efficient reciprocity-based computation of EEG forward solutions [9].

Volume conduction modeling under quasi-static assumptions requires the solution of Poisson's equation on a geometric representation of the human head. Early head conductor models used concentric spheres to represent different electrically homogeneous tissue types (e.g., scalp, skull, and brain; [10]) and offers closed form solutions that are analytically computable. However, spherical models provide only a rough geometric approximation, and cannot incorporate the spatially varying, potentially anisotropic conductivities that are present in the head. Capturing the complex features of arbitrary head tissues and conductivities [2, 5, 11] requires discretized tissue geometries that combine spatial locations (nodes) and their connections (elements) to form meshes. These meshes can describe regular grids, or be algorithmically generated to adapt to geometric and conductivity requirements [2]. Unlike spherical models, closed form solutions do not exist in these geometries, necessitating the use of numeric solution methods. We focus here on three commonly used numerical approaches for realistic head modeling: the finite element method (FEM), the finite difference method (FDM), and the boundary element method (BEM).

Of those three approaches, the finite element method (FEM) is the mostly adaptable numerical method that can efficiently capture arbitrary geometries and conductivity distributions. The volume is typically subdivided into non-overlapping tetrahedral or hexahedral elements with solved voltage potentials interpolated within each element. This allows smooth tissue boundaries to be modeled, and adaptive meshing to reduce node density within large homogeneous regions, thereby reducing overall computational requirements.

By contrast, the finite difference method (FDM) is more easily implemented, but more computationally expensive when modeling complex head geometries. The computational mesh must be structured as a regular grid in order to construct valid difference equations at all points. Thus doubling spatial resolution in all directions produces an 8-fold increase in the number of computational nodes, regardless of tissue homogeneity. Additionally, restricting the computational geometry to a grid means boundary layers between tissue types will take on a stair-step appearance that may not accurately represent realistic tissue boundaries.

In contrast to FDM/FEM, the boundary element method (BEM) solves Poisson's equation using triangulated surfaces describing the interface layers of head tissues and assumes homogeneous conductivity distributions within [12]. A system matrix is generated to describe the relationship between voltage potentials and normal current vectors on these surfaces. Arbitrary source and sensor locations can be modeled with appropriately generated interpolation matrices mapping sources and sensors to the points associated with this head matrix.

Each of these numerical methods have strengths and weaknesses with regard to the complexity of implementation, the accuracy of the resulting solutions, and the amount of computation required to obtain them. While these numerical techniques have all been demonstrated to be accurate with respect to a spherical shell model [13, 14, 15], to our knowledge they have not been compared to one another in the context of modeling more

complex head geometries. An understanding of how these methods differ from one another is important in practical applications regarding accuracy and computational complexity.

In this study, we construct a patient-specific head segmentation including hard and soft skull bone, gray and white matter, cerebrospinal fluid (CSF) and scalp tissue, and compare the relative numerical accuracy of FEM, FDM, and BEM approaches to one another. Using metrics of differences in topography and magnitude, we evaluate the relative performance of each technique, with and without anisotropic conductivities when supported by the approach. Our results suggest that the FEM and FDM techniques produce highly similar answers within the brain, while the BEM, which cannot incorporate tissue anisotropies or complex tissue geometries, produces significantly higher relative errors.

## 2. Methods

### 2.1. Data Collection and Initial Processing

T1, T2, and diffusion weighted MRI scans were obtained from a 14 year old control subject using a Siemens Magnetom 3T scanner. The imaging protocol included 3d MPRAGE T1 (1 mm isotropic resolution, 176 × 220 × 220 voxels) and T2TSE (1 mm resolution) structural scans. A 45 direction CUSP scan (2 mm isotropic resolution) was used to collect diffusion data, with tensors estimated using robust least squares. All images were coregistered to a common reference frame, and resampled to the 1 mm resolution of the T1 scan.

A seven tissue segmentation of the head was generated using a combination of automated methods and manual segmentation. A multi-atlas statistical segmentation approach was used to identify the intracranial cavity, and the grey matter, white matter, and cerebrospinal fluid regions therein [16]. Scalp tissue was segmented using a threshold approach followed by manual adjustments for MRI measurement noise and goggles/headphones. The skull was similarly extracted using thresholding, image processing operations (e.g., dilate, erode, etc.), and manual adjustments. Soft skull bone and sinus cavities were identified by thresholding within the skull compartment.

Conductivities for each tissue type in the segmentation were assigned using values established in the literature [4]. Scalp tissue was assigned a isotropic conductivity of 0.43 S/m, hard bone to 0.064 S/m, soft bone to 0.0268 S/m, and sinuses to 1e-6 S/m. Within the intracranial cavity, cerebrospinal fluid was assigned a conductivity of 1.79 S/m, gray matter to 0.33 S/m, and white matter to 0.142 S/m for the isotropic model. To incorporate anisotropic conductivities within the white matter region, diffusion MRI was used to compute individual anisotropic conductivity tensors within each voxel [17]. In conjunction with the head segmentation described above, two separate three dimensional distributions of tissue conductivity are available: one with isotropic conductivities in all tissues, and one with anisotropic conductivities only for white matter tissue.

### 2.2. Numerical Modeling Approaches

**Finite Element Method (FEM)—**Based on the head tissue segmentation, each voxel that belongs to a head tissue was subdivided into 5 tetrahedral elements. The final tetrahedral mesh contained $18.8\times10^6/3.7\times10^6$ elements/nodes. The mesh was used in two variants,

$FEM_i$ and $FEM_a$, whereas isotropic and (an)isotropic conductivity tensors where assigned to tetrahedral mesh elements respectively.

**Finite Difference Method (FDM)—**We constructed finite difference models from the isotropic and anisotropic conductivity images using an approach that employs transition layers to permit arbitrary anisotropic conductivities within each individual voxel [18]. This approach places computational nodes at the corners of each volume element, and was constructed at the full 1 mm isotropic resolution of the structural MRI, resulting in a hexahedral mesh with $3.7 \times 10^6/3.8 \times 10^6$ elements/nodes respectively. Similar to FEM, for the final FDM mesh, two versions were generated ($FDM_i$ and $FDM_a$).

**Boundary Element Method (BEM)—**The boundary element method was implemented using the software tools available from the OpenMEEG project (http://openmeeg.github.io). The model was constructed by identifying three surfaces [19], located at the interfaces between scalp and air, skull and scalp, and intracranial cavity and skull. Tissues conductivities were assigned as 0.43 S/m for the scalp domain, 0.01 S/m for the skull domain, and 0.33 S/m within the brain. The symmetric BEM matrix was constructed, as well as the matrices necessary to appropriately map internal voltages on a 1mm grid and scalp injection currents at electrode locations to the BEM surfaces.

### 2.3. FDM/FEM/BEM - Forward problem

Despite methodological differences, each of these techniques requires solution of a linear system of equations to obtain interior voltage distributions as $A \cdot x = b$, with A being the forward problem matrix, $x$ denoting a vector of voltage potentials at each computational node, and $b$ representing the current intensities injected on the scalp surface. Solutions to the resulting linear inverse problems were computed using SCIRun [20] with the MINRES algorithm (Jacobi preconditioning), and allowed to converge to a relative error of $10^{-9}$. Solutions were obtained for each of 72 electrode locations corresponding to the standard 10-10 electrode configuration, with electrode Cz used as the common reference.

## 3. Results

A total of five head models were constructed for comparison: four modeling (an)isotropic conductivity distributions for finite element and difference method ($FEM_i$, $FEM_a$, $FDM_i$, $FDM_a$) as well as a $BEM$ model featuring 3 layers of isotropic conductivities. The current injection problem was solved for each electrode in a standard 10-10 array (72 times), using Cz as the fixed reference electrode. A map of nodal voltages was computed for each model and current injection electrode pair. The relative changes in voltage distribution between models were evaluated using the relative difference metric (RDM), which measures changes in voltage topography, and the magnitude difference (MAG), which measures changes in overall signal magnitude ([21]). For each spatial location, these metrics were computed across all electrode pairs to describe overall modelling accuracy at that spatial location.

Figure 1 summarizes the differences for each possible pairing of numerical models using histograms of RDM and MAG. For a better visual assessment, the (min,max) range of voltage values (x-axis) in FEM/FDM have been depicted to be identical in contrast to higher

errors achieved with BEM. The lowest errors are seen when comparing the isotropic and anisotropic versions of the FEM and FDM methods. For all comparisons, the BEM model shows significantly higher RDM and MAG errors than the other models, which reflects the increased simplicity necessary to generate a boundary based approach. The BEM model lacks the highly conductive CSF region, and additionally does not differentiate between hard bone, soft bone, and sinus regions. Even provided a high resolution segmentation, identification of sufficiently accurate non-intersecting boundary models for each of these regions is highly challenging, and three surface models are the most commonly employed BEM configuration.

The spatial distribution of the RDM is displayed in Figure 2. For the $FEM_i$, $FDM_a$, $FDM_i$, and *BEM* models, voltages were compared to the $FEM_a$ model in terms of RDM. These images demonstrate several common features seen in the computed relative differences. First, using isotropic conductivities, both the FEM and FDM methods produce increased RDM throughout the brain, in particular for deeply located points near the brain stem. The BEM model shows a similar spatial pattern, however, as seen in the histograms above, these differences are on average much higher than those seen between the FEM and FDM models. Peak differences for the two FDM models are seen within the scalp region, immediately adjacent to electrode locations, however these do not translate to local peaks within brain tissue due to volume conduction effects of skull/CSF (as visualized in [4]).

Of additional note are the errors seen across all models in the corpus callosum. The white matter is highly anisotropic in this region, producing spatial inhomogeneity in the conductivity. The errors are, however, also localized to the corpus callosum, and unlikely to significantly impact simulated EEG or TCS voltage potentials.

A corresponding set of slices depicting computed MAG values are presented in Figure 3. With both the FEM and FDM approaches, the models using anisotropic conductivity can be seen to exhibit smooth and spatially similar magnitude differences across the cortex. These values are greatest for deep locations near the brainstem. Both isotropic and anisotropic finite difference models show additional magnitude differences within the scalp tissue. These values correspond spatially to those seen in the RDM images, and result from the FDM computing significantly higher voltages at the computational nodes immediately adjacent to current injection points. These results suggest that, assuming FEM to be the more accurate approach, the FDM model may not be well suited to computational scenarios where sensitivities/voltages need to be accurately computed near electrode locations. Finally, similar to RDM, the BEM model shows significantly higher relative magnitude differences than the FEM and FDM models, with the largest errors located primarily within the skull and brain stem.

## 4. Conclusions

We have presented a comparison of three numerical approaches to modeling bioelectric propagation in a complex head model by evaluating maps of voltage potential computed for the current injection problem. Both the finite element and finite difference approaches produce voltage distributions which are highly similar, while the boundary element approach

shows consistent differences in voltage intensities and produces larger topographic errors than the other methods. While careful construction of additional tissue boundary meshes may improve BEM accuracy, this is a difficult problem that complicates widespread routine use. The FEM and FDM, by contrast, can easily be constructed on a computational grid that matches available structural imaging, making implementation of these methods relatively straightforward. With the increasing availability of high quality MRI imaging and associated high resolution image segmentations, patient-specific bioelectric models incorporating this additional knowledge should become the standard for both research and clinical use.

## Acknowledgments

This project was supported by the National Institute of General Medical Sciences of the National Institutes of Health under grant number P41 GM103545-17, and the National Institute of Neurological Disorders and Stroke, grant number K25NS067068.

## References

1. Dannhauer, Moritz, Lämmel, Eric, Wolters, Carsten H., Knösche, Thomas R. Spatio-temporal regularization in linear distributed source reconstruction from eeg/meg: a critical evaluation. Brain topography. 2013; 26(2):229–246. [PubMed: 23112100]
2. Rullmann M, Anwander A, Dannhauer M, Warfield SK, Duffy FH, Wolters CH. EEG source analysis of epileptiform activity using a 1mm anisotropic hexahedra finite element head model. 2009; 42(2):399–410.
3. Nitsche MA, Cohen LG, Wassermann EM, Priori A, Lang N, Antal A, Paulus W, Hummel F, Boggio PS, Fregni F. Transcranial direct current stimulation: State of the art 2008. 2008; 1(3):206–223.
4. Eichelbaum S, Dannhauer M, Hlawitschka M, Brooks D, Knösche TR, Scheuermann G. Visualizing simulated electrical fields from electroencephalography and transcranial electric brain stimulation: a comparative evaluation. NeuroImage. 2014; 101:513–30. [PubMed: 24821532]
5. Dannhauer M, Lanfer B, Wolters CH, Knösche TR. Modeling of the human skull in EEG source analysis. Human Brain Mapping. 2011; 32(9):1383–99. [PubMed: 20690140]
6. Dannhauer M, Brooks D, Tucker D, MacLeod R. A pipeline for the simulation of transcranial direct current stimulation for realistic human head models using scirun/biomesh3d. Conference proceedings:… Annual International Conference of the IEEE Engineering in Medicine and Biology Society IEEE Engineering in Medicine and Biology Society Conference. 2012; 2012
7. Guler S, Dannhauer M, Erem B, MacLeod R, Tucker D, Turovets S, Luu P, Meleis W, Brooks DH. Optimizing stimulus patterns for dense array tdcs with fewer sources than electrodes using a branch and bound algorithm. International Symposium on Biomedical Imaging (ISBI), to be held at the Clarion Congress Hotel in Prague, Czech Republic, April 13-16, 2016. 2016; 2016
8. Nitsche MA, Boggio PS, Fregni F, Pascual-Leone A. Treatment of depression with transcranial direct current stimulation (tDCS): a review. Experimental neurology. 2009; 219(1):14–19. [PubMed: 19348793]
9. Ziegler, Erik, Chellappa, Sarah L., Gaggioni, Giulia, Ly, Julien QM., Vandewalle, Gilles, André, Elodie, Christophe, Geuzaine, Phillips, Christophe. A finite-element reciprocity solution for EEG forward modeling with realistic individual head models. NeuroImage. Dec.2014 103:542–551. [PubMed: 25204867]
10. de Munck JC. The potential distribution in a layered anisotropic spheroidal volume conductor. J Appl Phys. 1988; 64(2):464–470.
11. Fiederer LDJ, Vorwerk J, Lucka F, Dannhauer M, Yang S, Dmpelmann M, Schulze-Bonhage A, Aertsen A, Speck O, Wolters CH, Ball T. The role of blood vessels in high-resolution volume conductor head modeling of {EEG}. NeuroImage. 2016; 128:193–208. [PubMed: 26747748]
12. Hallez, Hans, Vanrumste, Bart, Grech, Roberta, Muscat, Joseph, de Clercq, Wim, Vergult, Anneleen, D'Asseler, Yves, Camilleri, Kenneth P., Fabri, Simon G., van Huffel, Sabine, Lemahieu,

Ignace. Review on solving the forward problem in EEG source analysis. Journal of neuroengineering and rehabilitation. 2007; 4:46. [PubMed: 18053144]

13. Gramfort A, Papadopoulo T, Olivi E, Clerc M. Forward field computation with openmeeg. Computational Intelligence and Neuroscience. 2011; 2011
14. Wolters CH, Kstler H, Mller C, Hrdtlein J, Anwander A. Numerical approaches for dipole modeling in finite element method based source analysis. International Congress Series. 2007; 1300:189–192.
15. Jing, Li, Zhu, Shanan, He, Bin. A finite difference method for solving the three-dimensional eeg forward problem; Engineering in Medicine and Biology Society, 2005 IEEE-EMBS 2005 27th Annual International Conference of the; 2005. p. 1540-1543.
16. Weisenfeld, Neil I., Warfield, Simon K. Automatic segmentation of newborn brain MRI. NeuroImage. 2009; 47(2):564–572. [PubMed: 19409502]
17. Tuch DS, Wedeen VJ, Dale AM, George JS, Belliveau JW. Conductivity tensor mapping of the human brain using diffusion tensor MRI. Proceedings of the National Academy of Sciences of the United States of America. Sep; 2001 98(20):11697–11701. [PubMed: 11573005]
18. Saleheen HI, Ng KT. New finite difference formulations for general inhomogeneous anisotropic bioelectric problems. IEEE Transactions on Biomedical Engineering. Sep; 1997 44(9):800–809. [PubMed: 9282472]
19. Tadel F, Baillet S, Mosher JC, Pantazis D, Leahy RM. Brainstorm: A user-friendly application for meg/eeg analysis. Computational Intelligence and Neuroscience. 2011; 2011
20. SCIRun. scientific computing and imaging institute, university of utah; Scirun: A scientific computing problem solving environment. http://www.scirun.org
21. Lanfer B, Scherg M, Dannhauer M, Knoesche TR, Burger M, Wolters CH. Influences of skull segmentation inaccuracies on EEG source analysis. 2012; 62(1):418–31.

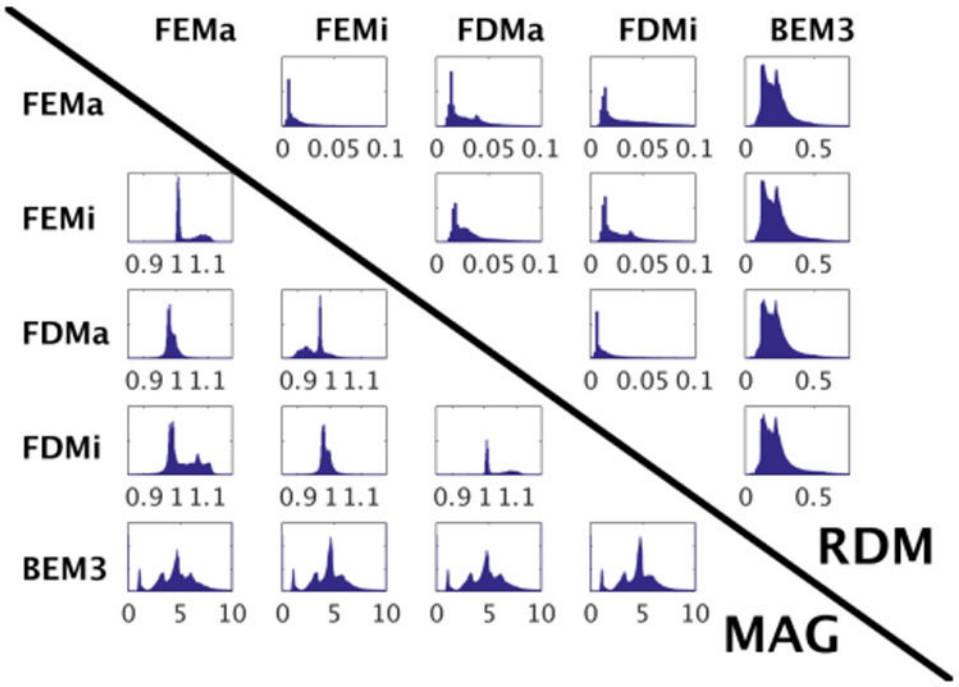


**Fig. 1.**

Histogram plots of RDM and MAG error across the entire head. RDM plots are in the upper triangle, MAG plots in the lower.

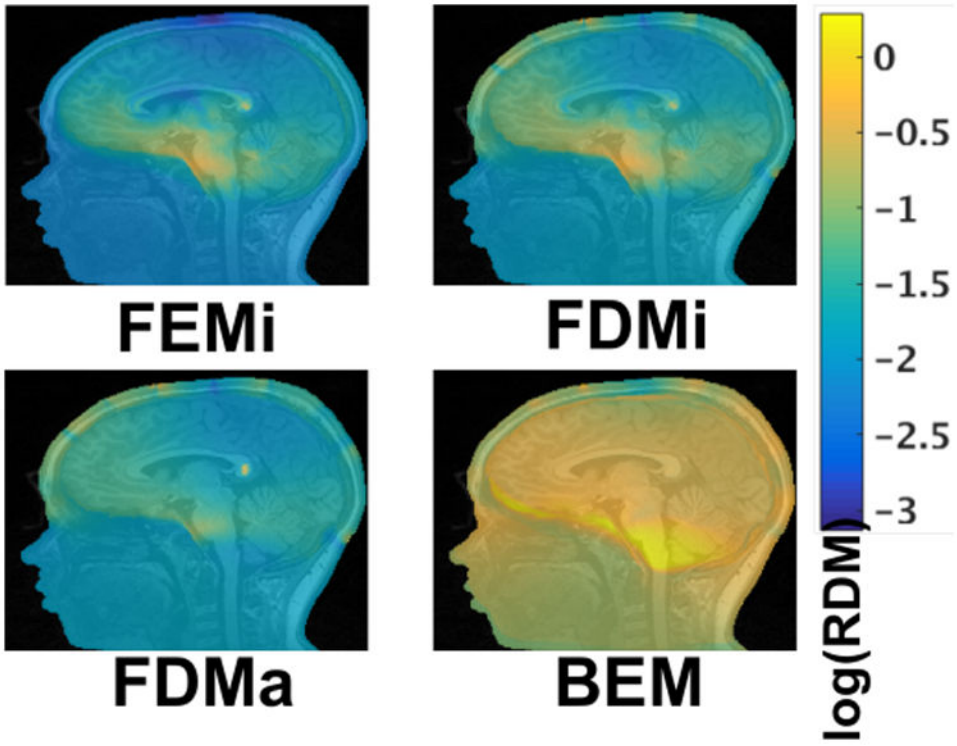


**Fig. 2.**
Relative topographic differences (RDM) as compared to the $FEM_a$ model.

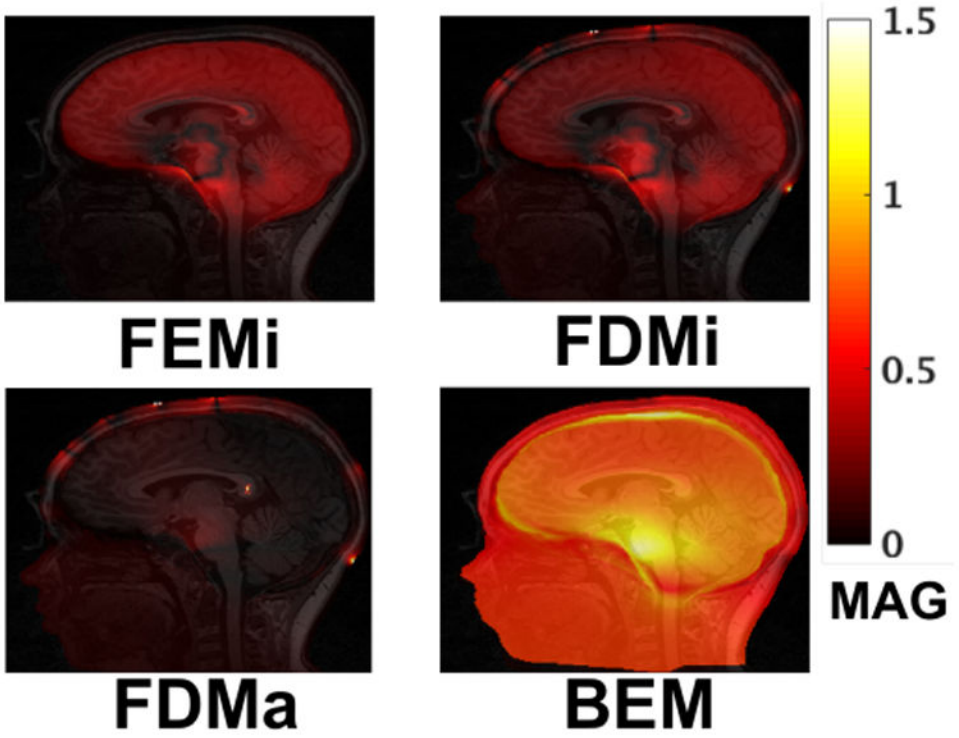


**Fig. 3.**

Relative MAG as compared to the $FEM_a$ model. Displayed MAG values were recomputed as $exp(abs(log(MAG))) \in [1, inf]$ to better visualize relative changes.